Assessment of the metawedge as a mitigation measure for railway induced ground vibration

Bracci, Alessandro; Fărăgău, Andrei; Metrikine, Andrei; van Dalen, Karel; Corradi, Roberto; Vlijm, Eliam

DOI
10.1088/1742-6596/2647/20/202003

Publication date
2024

Document Version
Final published version

Published in
Journal of Physics: Conference Series

Journal of Physics: Conference Series

PAPER • OPEN ACCESS

Assessment of the metawedge as a mitigation measure for railway induced ground vibration

To cite this article: Alessandro Bracci *et al* 2024 *J. Phys.: Conf. Ser.* **2647** 202003

Journal of Physics: Conference Series **2647** (2024) 202003 doi:10.1088/1742-6596/2647/20/202003

Assessment of the metawedge as a mitigation measure for railway induced ground vibration

Alessandro Bracci[1], Andrei Fărăgău[2], Andrei Metrikine[2], Karel van Dalen[2], Roberto Corradi[1], and Eliam Vlijm[3]

[1]Politecnico di Milano, Department of Mechanical Engineering, Piazza Leonardo da Vinci 32, 20133, Milan, Italy

[2]Delft University of Technology, Department of Engineering Structures, Mekelweg 5, 2628 CD Delft, Netherlands

[3]Cohere Consultants, Bergstraat 29, 3811 NE Amersfoort, Netherlands

E-mail: `alessandro.bracci1997@gmail.com`

Abstract. Railway induced ground vibrations are of increasing importance for structures and inhabitants in the vicinity of railway tracks. This study investigates the capabilities of a novel mitigation measure, a so-called metawedge, in reducing the ground-borne vibration at the receiver end. A metawedge is series of barriers (i.e., resonators) arranged periodically in the longitudinal direction and each one is offset with respect to the others in depth direction (i.e., while the first barrier is completely on the surface, the last barrier can be completely embedded). The advantage of this countermeasure is that it can convert the incoming Rayleigh (surface) waves into body ones, redirecting the energy content deep into the ground. Simulation results show that the metawedge is capable of significantly reducing the vibration levels with as few as five resonators. Furthermore, while conventional single trenches are efficient as mitigation measures only at a certain angle of the incoming waves (outside the critical cone), the metawedge is efficient inside this cone. Although the metawedge solution is promising, this paper serves solely as a proof of concept, and additional studies are necessary to design realistic resonators that can comply with the low frequencies of the railway induced ground vibrations. Nonetheless, this study shows that metamaterials-inspired solutions can play an important role in addressing present and future challenges of the railway transportation.

1. Introduction

Railway transportation is receiving increased attention due to it having the lowest percentage of green-house gasses emission in the transportation sector and its capability of running fully on electricity, making it an environmentally friendly mode of transportation. However, with this increasing demand, the previously considered acceptable problems surrounding railway transportation are quickly turning into challenging problems causing disruptions to the normal operation of traffic. One such an issue is the ground-borne vibration that is generated by, for example, wheel and rail unevenness, parametric excitation due to sleeper periodicity [1], or abrupt changes in the track's mechanical properties (i.e., transition zones [2–4]).

Mitigation measures for ground-borne vibration range from interventions at the source level (i.e., vehicle-structure interaction), at the receiver location (e.g., vibration isolating foundations), and on the transmission path. This work is concerned with the last category. Two of the most widespread mitigation measures are open (or soft in-filled) and the stiff in-filled trenches [1] that aim at hindering the wave transmission from source to receiver. The former countermeasure can prove efficient if the filling material is soft compared to the surrounding soil [5] and it has been experimentally confirmed that the measure is inefficient if the aforementioned condition is not satisfied [6]. Consequently, for railways on soft soils where the ground-borne vibrations are exacerbated an open trench (i.e., no filling material) is necessary to ensure its efficiency; this poses limitations in terms of trench depth and side-wall stability. The latter countermeasure, the stiff in-filled trench does not have this drawback and has been shown to be effective both theoretically [7] and experimentally [8]. However, its transmission reduction is only effective above a specific incidence angle of the incoming wave, below which it has a negligible influence on the wave transmission [7]. Consequently, this study aims to overcome both limitations of the two aforementioned countermeasures by investigating the capabilities of a novel mitigation measure, a so-called metawedge [9], in reducing the ground-borne vibration at the receiver end.

The application of metamaterials in elastic media allows guiding and controlling the wave propagation direction through the so-called wave-mode conversion mechanism. This concept, derived from photonic and phononic crystals, leads to innovative mitigation measures to attenuate the far-field vibrations generated by the surface waves [9]. A metawedge is composed of a series of barriers (i.e., resonators) arranged periodically in the longitudinal direction, but unlike traditional metamaterials, each resonator presents an offset with respect to the others in the depth direction (see Fig. 1). For example, the first resonator can lie on the soil surface (thus also acting as a noise barrier) while the last resonator can be completely embedded. The metawedge could be efficient at small incidence angles of the incoming wave, while the last barrier, which is completely embedded, can act as a traditional in-filled trench which is efficient at larger incident angles. A traditional metamaterial (i.e., without the embedment gradient), can also be efficient at blocking the wave transmission as shown for periodic geofoam-filled trenches [10] and periodic pile barriers [11]. However, in these cases most energy content would be reflected towards the source, potentially causing a negative feedback loop (increased vehicle vibration leading to stronger wave radiation) and to increased railway track wear. The metawedge, on the other hand, can convert the incoming surface waves into body ones due to its embedment gradient, re-directing the energy content deep into the ground. The potential drawback of this countermeasure is that the body waves can reflect from the interface between soil layers be re-directed towards the receiver.

The novelty of this paper lies in investigating the potential of the metawedge, which was previously introduced in earthquake engineering applications [9], as a possible mitigation measure for railway ground-borne vibrations. To this end, both a 2-D plane-strain model and, unlike most studies on the metawedge concept, a so-called 2.5-D model are employed, allowing to investigate the efficiency of the metawedge inside the conical region where the stiff in-filled trench performs poorly [12]. The soil is modelled as a homogeneous half-space meaning that the aforementioned potential drawback is excluded from this analysis. Although this should be investigated in future studies, the simplified soil model facilitates the initial investigation. This novel countermeasure where the first resonator can also fulfill the role of a noise barrier while the last one can incorporate the advantages of the stiff trench can prove to become a superior alternative to the traditional countermeasures for both the air- and ground-borne vibrations.

2. Model formulation and the metawedge design methodology

To investigate the performance of the metawedge, this paper makes use of two models: (i) a 2-D plane-strain model (a schematic figure is presented in Fig. 1) and (ii) a so-called 2.5-D model, which is basically a 3-D model that is homogeneous in the third direction (the direction of train motion). The former model is used for the preliminary design and assessment of the metawedge while the latter model allows to investigate the efficiency of the metawedge for incoming waves with varying different incidence angles. In both these models, the soil is modelled as a homogeneous half-space while the excitation is represented by a non-moving harmonic point load, as presented in Fig. 1. The railway track is not modelled, and although it can influence the quantitative results, its effect on the proof of concept is considered negligible.

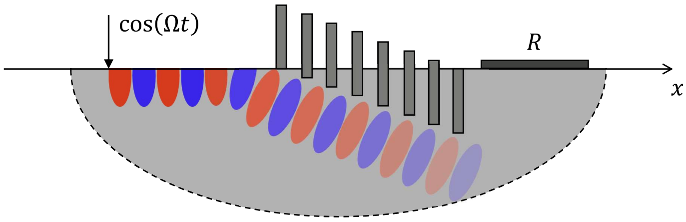

Figure 1: A schematic depiction of the problem considered: a harmonic load acting at the surface of a homogeneous half-space where a metawedge is placed between the source and the receiver.

The response of the formulated models is obtained by using a coupled boundary-element (BE), finite-element (FE), and thin-layer (TL) methods where the resonators are modelled with FE while the soil is modelled through TL and BE. The solution method is implemented in the FEMIX software (http://alvaroazevedo.com/femix/) developed by de Oliveira Barbosa and his collaborators [13]. The solution method formulation is thoroughly described in Refs. [13] and its practical potential in studying ground-borne vibration in Ref. [14].

Metawedge design methodology

The procedure through which the metawedge is designed is divided into three main parts. Firstly, the unit cell is designed as part of a structure composed of an infinite number of identical cells (see Fig. 2a) such that one of its band gaps coincides with the desired frequency range. Secondly, the designed unit cell is implemented in the 2-D model where the embedment gradient is imposed. The purpose of this step is to choose the gradient and number of necessary cells such that the optimum mitigation is obtained. Thirdly, the designed metawedge is implemented in the 2.5-D model to investigate the effect of the incidence angle of the incoming wave on the performance of the metawedge. An iteration between these three steps could be necessary to ensure the optimum design of the metawedge. In the following, the first step is elaborated.

The unit cell including one partially embedded resonator (Fig. 2b) is preliminary designed as part of a structure composed of an infinite number of identical cells (i.e., the gradient of the metawedge is neglected), as shown in Fig. 2a. The soil column is part of the metamaterial following the approach adopted in [15]. The properties of the unit cell are chosen to ensure that the band gap is at the desired frequency and its range is as large as possible.

The dispersion relation problem of an infinite periodic system can be transferred into an eigenvalue problem of a typical unit cell [10]. The dispersion curve of the periodic structure is determined by the wave vector in the first Brillouin zone. The eigenvalue problem is solved using a 2-D FEM model of the unit cell implemented in COMSOL Multiphysics version 5.4. An example is presented in Fig. 2c. The soil column depth H must be large enough to accurately represent the semi-infinite layer through a finite one. For Rayleigh waves, the motion is localized near the surface, which is about twice the wavelength of the surface waves. Therefore, H is chosen larger than three maximum Rayleigh wavelengths ($H > 3\lambda_{R,max}$), as imposed in [15]. The term $\lambda_{R,max}$ corresponds to the minimum frequency value f_{min}, which is set to 1 Hz for all the presented simulations. This ensures that $\mathbf{u} \approx \mathbf{0}$ at $z = -H$. Stress-free boundary conditions are used at the soil surface ($z = 0$), while the Floquet periodicity is imposed between unit cells (see Fig. 2c).

Once the dispersion relation is found, the surface modes must be distinguished from the bulk

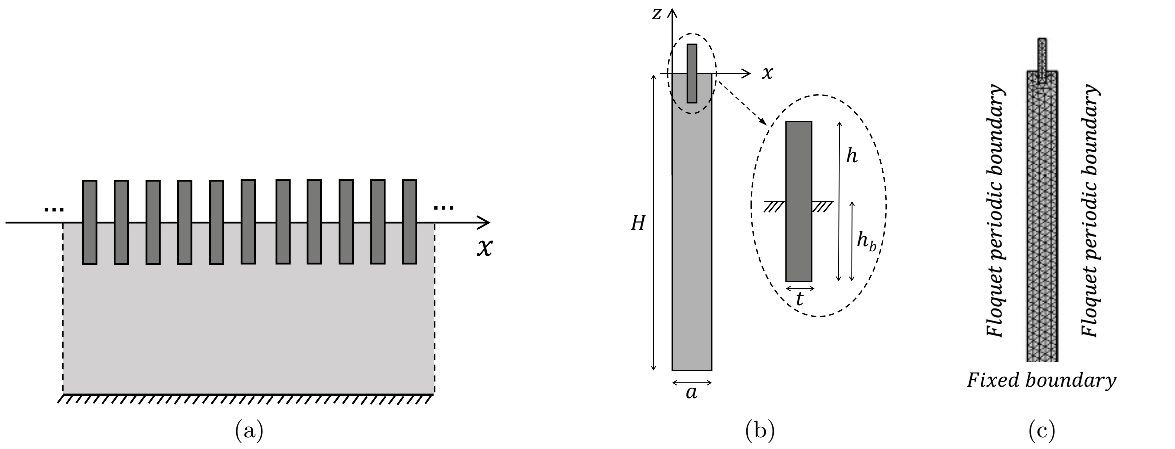

Figure 2: Schematic representation of the periodic metabarrier with partially embedded resonators used for designing the unit cell (a), unit cell (b), and FEM model of the unit cell (c).

ones. The distinction is made using the energy distribution parameter ξ [16], which reads

$$\xi = \frac{\int_{-2\lambda}^{0} \int_{0}^{a} W_\varepsilon \, dx \, dz}{\int_{-H}^{0} \int_{0}^{a} W_\varepsilon \, dx \, dz}, \tag{1}$$

where W_ε represents the elastic strain energy density. The surface integrals are computed for the soil column of the unit cell for its width a along the x-axis and for the depth values 2λ and H along the z-axis, as shown in Fig. 2b. Parameter ξ has a clear physical meaning representing the specific energy content located within two wavelengths for the examined wave mode. The surface modes are identified for $\xi > 90\,\%$ [16]. Once the surface modes are found, the corresponding band gaps along the first Brillouin zone are revealed (see Fig. 3).

3. Results and discussion

To propose an innovative countermeasure as a practically feasible solution, some realistic design constraints must be set. We focus the study on the ground-borne vibrations induced by cargo trains in tracks founded on soft soils. Shielding nearby buildings from vibrations generated by cargo trains is especially difficult due to their extremely low frequency content. Field measurements performed in Tricht, the Netherlands (reported in [12]), show that the main energy content is in the 5–10 Hz range, with specifically high energy content at around 6 Hz. This section investigates the metawedge performance for the aforementioned scenario.

To this end, a unit vertical point harmonic force is applied 60 m from the first unit cell of the metawedge. The receiver points are located at the soil surface between $120\,\text{m} < x < 160\,\text{m}$ from the source. The soil properties are chosen to qualitatively represent the aforementioned Tricht site with the mass density $\rho = 1700\,\text{kg/m}^3$, Young's modulus $E = 15\,\text{MPa}$, and Poisson's ratio $\nu = 0.40$. A very small soil damping ratio is chosen (i.e., 0.5 %), to emphasize the metawedge performance in the absence of strong material damping.

3.1. Proposed metawedge design

The metawedge design should be as compact as possible, to allow the development of a practically feasible structure that is not strongly intrusive in an urban area [17]. The proposed solution has five partially embedded resonators (see bottom panel of Fig. 6). Starting from the unit cell, the selected resonator board is characterized by a thickness $t = 0.2\,\text{m}$ and a total height $h = 3\,\text{m}$.

The soil part of the unit cell has thickness $a = 2\,\text{m}$ and total depth $H = 240\,\text{m}$. Steel has been chosen for the resonator material with density $\rho = 7830\,\text{kg/m}^3$, Young's modulus $E = 200\,\text{GPa}$, and Poisson's ratio $\nu = 0.26$ [15].

Following the design procedure described in Section 2, the dispersion curves of the surface waves are determined and presented in Fig. 3 for the embedded length $h_b = 0.4\,\text{m}$. The vibration modes of the unit cell manipulate the wave propagation in the medium through the Rayleigh mode hybridization with the surface resonances [18]. Without the resonators, the dispersion curves reduce to those of bulk and surface Rayleigh waves, which are described by the straight black lines in Fig. 3. The first two natural frequencies of the unit cell (higher modes are not discussed here) correspond to the flexural and longitudinal modes (resented in the right side of the figure), and give rise to two distinct band-gaps (i.e., frequency ranges in which surface waves cannot propagate). For frequencies in these band-gaps, the Rayleigh waves are transformed into body waves [17]. This phenomenon generates the two separate branches of "hybrid" Rayleigh waves that asymptotically approach the band gaps from the bottom with a phase velocity lower than the Rayleigh wave velocity c_{R}. The band gap closes when the upper branch has the phase velocity equals c_{S}. Surface modes with phase velocity larger than the shear-wave velocity c_{S} cannot exist in the elastic medium.

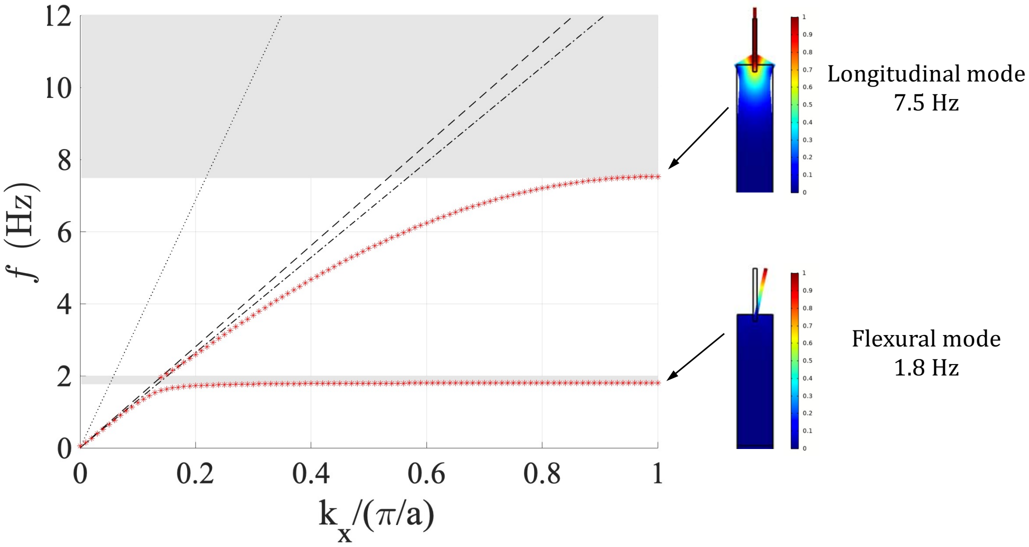

Figure 3: Dispersion curves of the surface wave (red star) for embedded length $h_b = 0.4\,\text{m}$, and the compressional (dotted line), shear (dashed line), and Rayleigh (dashed-dotted line) waves for the homogeneous half-space.

Fig. 3 shows that although the Rayleigh wave excites both the flexural and longitudinal modes of the metawedge, only the longitudinal one is able to activate a considerable band gap. Depending on the unit cell geometry and properties, the flexural mode plays a more or less marginal role. It appears extremely narrow for this specific case (about $1.8 - 2\,\text{Hz}$). Some authors directly neglect the contribution of the first resonance [9, 19]. Above the longitudinal mode, the second band gap appears wider due to the better wave and mode coupling with the vertical component of the Rayleigh wave [20].

The band gaps are manipulated by adjusting the embedded depth of the barriers along the x-axis. This layout guarantees that the mitigation mechanism of the countermeasure is dominated by the wave-mode conversion of Rayleigh waves into bulk ones, as demonstrated in

[19]. In particular, the second band gap should be shifted to lower frequencies to reach at least the target value of 6 Hz. Surface waves should experience a clear conversion when this excitation frequency is imposed at the surface.

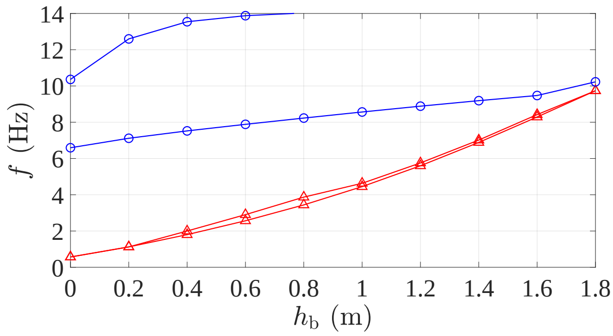

Figure 4: The first (red triangle) and second (blue circle) band gaps vs embedded length h_{b}.

The dispersion curves are determined for unit cells with several embedded depth values ($0\,\mathrm{m} \leq h_b \leq 1.8\,\mathrm{m}$). The evolution of the first two band gaps is presented as a function of h_b in Fig. 4. As indicated, the regions between the two equal curves express the interval of the band gaps. With this metawedge setup, the Rayleigh waves travelling from left to right experience an increasing h_b trend. It can be seen that the second band gap can reach smaller frequencies if h_b is decreased. Beginning with the first barrier with $h_b = 0$, the first five barriers with the embedded depth difference $\Delta h_b = 0.1\,\mathrm{m}$ are selected. This implies that the fifth barrier has $h_b = 0.4\,\mathrm{m}$ with the imposed metawedge slope of $\zeta = 0.05$.

3.2. Results from the 2-D model

The mitigation performance of the designed system is firstly assessed in the space-frequency domain under the plane strain assumption ($k_y = 0$). In other words, the plane wave motion is perpendicular to the metawedge. The efficiency of the mitigation measure is expressed through the so-called insertion loss IL_i which is the ratio between the response of the unmitigated U_i^{ref} and mitigated scenarios U_i, and is given by the following expression [7]:

$$\mathrm{IL}_i(x, z, \omega) = 20\log_{10}\frac{|U_i^{\mathrm{ref}}(x, z, \omega)|}{|U_i(x, z, \omega)|}, \quad i \in \{x, y, z\}. \tag{2}$$

Fig. 5a shows the vertical insertion loss IL_z at the soil surface for different excitation frequencies and horizontal positions. The system appears clearly effective in mitigating the vibration for $\omega > 2\pi \times 5\,\mathrm{Hz}$. Fig. 5b shows the insertion loss $\mathrm{IL}_{\mathrm{max}}$ computed with the maximum real part of the displacements occurring at the receiver positions. It depicts how the peak performance of the metawedge is achieved around 6 Hz, after a steep increase. The horizontal component of the soil response presents an almost identical reduction even though the response amplitudes are significantly lower (not presented here for brevity).

Fig. 5 confirms that the designed solution is able to mitigate ground-borne vibration following the design constraints previously recommended, at least for waves perpendicular to the metawedge. Furthermore, the wave-mode conversion mechanism is clearly visible in Fig. 6. The surface wave is redirected deep into the soil when it passes the metawedge, thus reducing the amplitude at the surface behind the barrier, as already indicated by Fig. 5. The advantageous effect of this countermeasure is evident when comparing the top and bottom panels in Fig. 6.

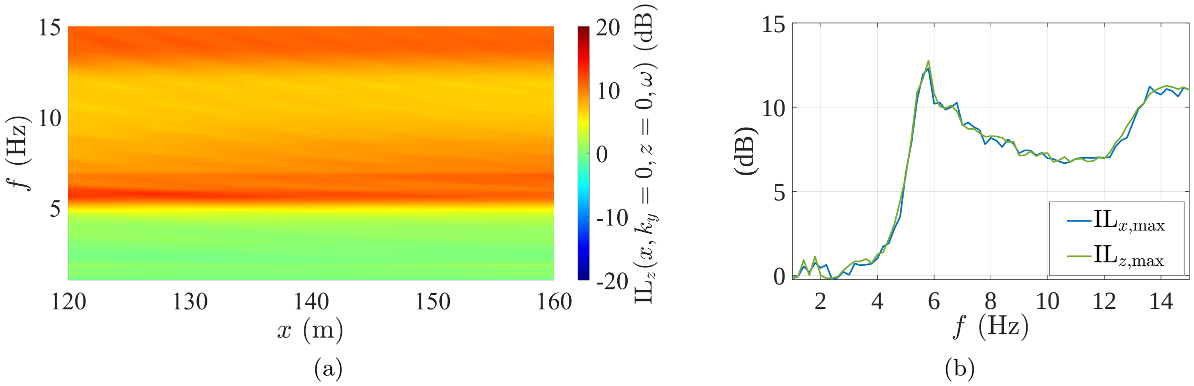

Figure 5: The vertical insertion loss at receiver position ($z = 0$ and $x \in [120, 160]$) vs frequency (panel a), and the maximum horizontal and vertical insertion losses vs frequency (panel b).

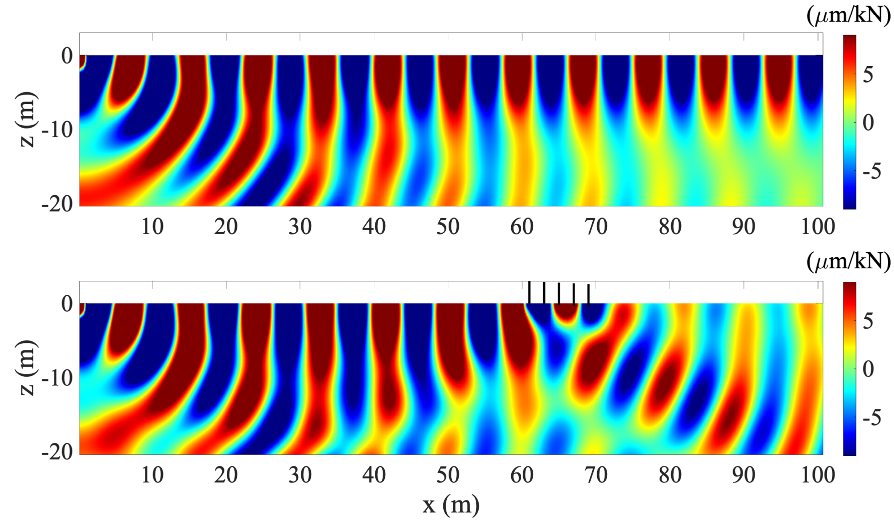

Figure 6: Real part of the vertical displacement $\mathrm{Re}(u_z(x, k_y = 0, z, \Omega = 2\pi \times 6\,\mathrm{Hz}))$ generated by vertical harmonic load in homogeneous soil (top panel) and with metawedge (bottom panel).

3.3. Influence of wave incidence angle–2.5-D model

Since the waves generated by trains approach the countermeasure at different incidence angles, it is important to investigate the influence of the incidence angle on the performance of the metawedge. This is done by using the 2.5-D model. Consequently, the insertion loss is now presented in the space-wavenumber (k_y in y-direction)-frequency domain.

Fig. 7 presents the vertical insertion loss IL_z for one receiver point at the soil surface and distance $x = 120\,\mathrm{m}$ from the source. On the vertical axis, $K_y = \frac{k_y}{\omega}$ is used to make the link between wavenumber k_y and the incidence angle θ, which is also presented on the right y-axis. As shown in the previous section, the countermeasure is effective only for frequencies larger than 5 Hz. When it comes to the incidence angle, the metawedge shows large insertion loss values in three ranges: (i) $\theta \approx$ 0–5 degrees, range in which the results are qualitatively the same as the ones presented in the previous section, (ii) $\theta \approx$ 10–20 degrees (exact range depends on the frequency), in which the insertion loss can be even larger than at small angles, and (ii) $\theta > 60$ degrees, for which the wave travels a much larger distance to reach the metawedge and, consequently, the soil damping plays an important role in the reduction observed. Moreover, the insertion loss is positive even outside these angle ranges with very few exceptions.

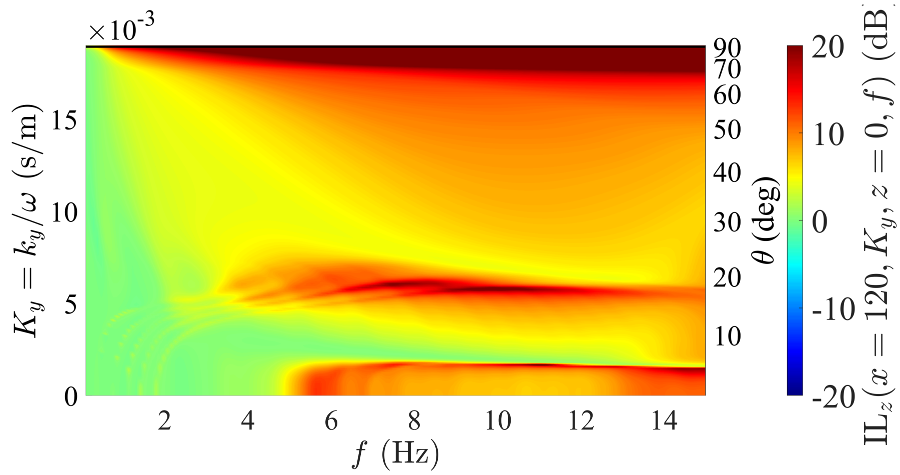

Figure 7: The vertical insertion loss vs frequency and incidence angle of the incoming wave.

Applying the inverse Fourier transform over wavenumber k_y, the soil response is expressed in the space-frequency domain. The vertical displacement field and the vertical insertion loss are plotted for $\Omega = 2\pi \times 6\,\mathrm{Hz}$ in Fig. 8a and Fig. 8b, respectively. To avoid cluttering the plots, only the embedded parts of the resonators are shown in Fig. 8b by the black bands.

The metawedge appears particularly effective in mitigating the vibration along the x-axis in the above-mentioned conical region behind the resonators. This aspect marks an important difference from the classical trench countermeasure, which generally shows poor performance below a certain critical incidence angle [7]. For some specific θ values, the metawedge seems unable to redirect the incoming wave deep into the ground. This is probably given by the different resonator properties that the incoming waves experience reaching the metawedge at $\theta > 0$. On the other hand, the wave-mode conversion phenomenon is clearly depicted in the xy-plane, where negative insertion loss zones appear for $z < -10\,\mathrm{m}$.

Fig. 8 shows that the metawedge is, to some extent, complementary to the stiff in-filled trench, where the stiffness effect could act where the wave-mode conversion mechanism does not appear effective. The complementary performance of the two different mitigation measures highlights how a hybrid solution could lead to nearly complete vibration mitigation at the surface. Indeed,

Conclusion

The paper investigated the performance of a novel mitigation measure, the so-called metawedge, for railway induced ground vibrations. By means of the wave-mode conversion mechanism, the proposed mitigation measure is able to convert the incoming surface waves into body waves exploiting the non-conventional dispersion properties of the resonators array. The potential of this countermeasure is investigated using a 2-D plane-strain model in which soil is modelled as a homogeneous half-space. The effect of the incident angle of the incoming wave on the performance of the metawedge is also analysed by using a 2.5-D model.

Results show that the proposed metawedge is successful in attenuating vibrations even at very low frequencies (i.e., $5 - 10\,\mathrm{Hz}$ typically generated by cargo trains). More importantly, the metawedge is most efficient at small-to-medium incident angles, at which traditional countermeasures such as the stiff trench are not. Although the metawedge design proposed in this paper is slightly unrealistic, it serves as a proof of concept. Future studies can investigate more realistic designs that do not compromise the efficiency of the countermeasure.

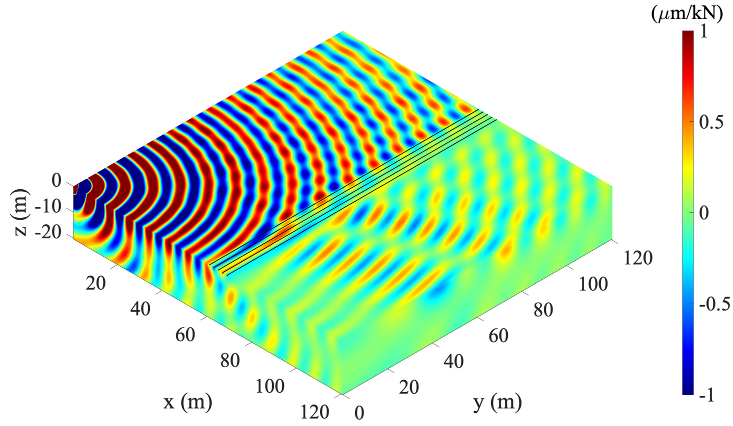

(a) $\mathrm{Re}(u_z(x, y, z, \Omega = 2\pi \times 6\,\mathrm{Hz}))$.

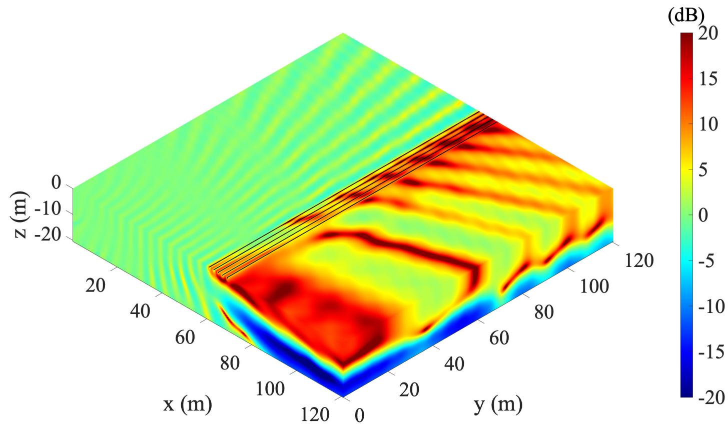

(b) $\mathrm{IL}_z(x, y, z, \Omega = 2\pi \times 6\,\mathrm{Hz})$.

Figure 8: The vertical displacement (a) and vertical insertion loss (b) generated by a unit harmonic vertical point load applied at $x = y = z = 0$.

If properly designed, the metawedge can represent an improved alternative to the stiff trench. Moreover, a superior performance could be achieved through a metawedge with the last resonator fully embedded, thus incorporating the benefits of the traditional stiff trench. Also, the first resonator being completely out of the ground could act as a noise barrier. Exploiting this aspect, the construction could act in a combined way, protecting the lineside residents from both ground- and air-borne vibration. Finally, further research is necessary to develop competitive solutions with focus on feasible and compact designs.

References

[1] G. Lombaert, G. Degrande, S. François, and D. J. Thompson. Ground-borne vibration due to railway traffic: A review of excitation mechanisms, prediction methods and mitigation measures, noise and vibration mitigation for rail transportation systems. In *Notes on Num. Fluid Mech. and Multidisc. Design*, pages 253–287. 2015.

[2] J. de Oliveira Barbosa, A. Fărăgău, and K. van Dalen. A lattice model for transition zones in ballasted railway tracks. *J. of Sound and Vibr.*, 494:115840, 2021.

[3] J. de Oliveira Barbosa, A. Fărăgău, K. van Dalen, and M. Steenbergen. Modelling ballast

via a non-linear lattice to assess its compaction behaviour at railway transition zones. *J. of Sound and Vibr.*, 530:116942, 2022.

[4] A. Fărăgău, , T. Mazilu, A. Metrikine, T. Lu, and K. van Dalen. Transition radiation in an infinite one-dimensional structure interacting with a moving oscillator—the green's function method. *J. of Sound and Vibr.*, 492:115804, 2021.

[5] D. J. Thompson, J. Jiang, M. G. R. Toward, M. Hussein, E. Ntotsios, A. Dijckmans, P. Coulier, G. Lombaert, and G. Degrande. Reducing railway-induced ground-borne vibration by using open trenches and soft-filled barriers. *Soil Dyn. and Earthquake Eng.*, 88:45–59, sep 2016.

[6] S. François, M. Schevenels, B. Thyssen, J. Borgions, and G. Degrande. Design and efficiency of a composite vibration isolating screen in soil. *Soil Dy. and Earthquake Eng.*, 39, 2012.

[7] P. Coulier, S. François, G. Degrande, and G. Lombaert. Subgrade stiffening next to the track as a wave impeding barrier for railway induced vibrations. *Soil Dyn. and Earthquake Eng.*, 48:119–131, may 2013.

[8] P. Coulier, V. Cuéllar, G. Degrande, and G. Lombaert. Experimental and numerical evaluation of the effectiveness of a stiff wave barrier in the soil. *Soil Dyn. and Earthquake Eng.*, 77:238–253, oct 2015.

[9] A. Colombi, P. Roux, S. Guenneau, P. Gueguen, and R. V. Craster. Forests as a natural seismic metamaterial: Rayleigh wave bandgaps induced by local resonances. *Scientific Reports*, 6(1), jan 2016.

[10] X. Pu, Z. Shi, and H. Xiang. Feasibility of ambient vibration screening by periodic geofoam-filled trenches. *Soil Dyn. and Earthquake Eng.*, 104:228–235, 2018.

[11] J. Huang, W. Liu, and Z. Shi. Surface-wave attenuation zone of layered periodic structures and feasible application in ground vibration reduction. *Construction and Building Materials*, 141:1–11, jun 2017.

[12] A. Bracci. Assessment of stiff trench and metawedge as mitigation measures for railway induced ground vibration. Master's thesis, Politecnico di Milano, 2022.

[13] J. de Oliveira Barbosa, E. Kausel, Á. Azevedo, and R. Calçada. Formulation of the boundary element method in the wavenumber–frequency domain based on the thin layer method. *Computers and Structures*, 161:1–16, 2015.

[14] J. de Oliveira Barbosa, P. Costa, and R. Calçada. Abatement of railway induced vibrations: Numerical comparison of trench solutions. *Engineering Analysis with Boundary Elements*, 55:122–139, 2015. Coupling Techniques.

[15] Z. Liu, K. Qin, and G. Yu. Partially Embedded Gradient Metabarrier: Broadband Shielding from Seismic Rayleigh Waves at Ultralow Frequencies. *Journal of Engineering Mechanics*, 146(5):04020032, may 2020.

[16] X. Pu and Z. Shi. A novel method for identifying surface waves in periodic structures. *Soil Dyn. and Earthquake Eng.*, 98:67–71, jul 2017.

[17] A. Palermo, S. Krödel, A. Marzani, and C. Daraio. Engineered metabarrier as shield from seismic surface waves. *Scientific Reports*, 6(1), dec 2016.

[18] M. Rupin, F. Lemoult, G. Lerosey, and P. Roux. Experimental demonstration of ordered and disordered multiresonant metamaterials for lamb waves. *Phys. Rev. Letrs.*, 112, 2014.

[19] Muhammad, T. Wu, and C. Lim. Forest Trees as Naturally Available Seismic Metamaterials: Low Frequency Rayleigh Wave with Extremely Wide Bandgaps. *International Journal of Structural Stability and Dynamics*, 20(14):2043014, 2020.

[20] Muhammad and C. Lim. Natural seismic metamaterials: the role of tree branches in the birth of Rayleigh wave bandgap for ground born vibration attenuation. *Trees*, 35(4), 2021.